Hindawi
Journal of Nanomaterials
Volume 2022, Article ID 3992590, 10 pages
https://doi.org/10.1155/2022/3992590

Research Article

Aggregation Effects on Entropy Generation Analysis for Nanofluid Flow over a Wedge with Thermal Radiation: A Numerical Investigation

Rabia Rehman,[1] **Hafiz Abdul Wahab**,[1] **Nawa Alshammari**,[2] **Umar Khan**,[1] **and Ilyas Khan**[3]

[1]*Department of Mathematics and Statistics, Hazara University, Mansehra, Pakistan*
[2]*Department of Basic Sciences, College of Science and Theoretical Studies, Saudi Electronic University, Riyadh 11673, Saudi Arabia*
[3]*Department of Mathematics, College of Science Al-Zulfi, Majmaah University, Al-Majmaah 11952, Saudi Arabia*

Correspondence should be addressed to Rabia Rehman; rabiarehman635@gmail.com

Received 18 October 2021; Revised 28 May 2022; Accepted 8 August 2022; Published 24 September 2022

Academic Editor: Anwar Saeed

The current study investigated the formation of entropy in a nanofluid flow in a wedge with thermal radiation and convective boundary conditions. Nanoparticle aggregation is also taken into consideration. The rate of heat transmission of a water-based aggregated fluid over a wedge has been investigated due to the effects of thermal radiation. A set of nonlinear differential equations governs the flow process, and these are numerically solved using a helpful approach called the Runge-Kutta-Fehlberg scheme. This method starts by breaking down the equations into a collection of first-order equations. The RK method then solves those equations. The effects on flow and heat transmission are studied using graphical analysis. Entropy generation and Bejan number changes are also graphically displayed, and the results are discussed in detail. These equations' answers were also incorporated into a dimensionless entropy generating equation. According to the findings, raising the radiation parameter and decreasing boundary convection minimize entropy generation, while nanoparticles boost entropy production.

1. Introduction

The "nanofluid" is characterized by conventional nanofluid papers as the scattering of solid nanoparticles, rods, and pipes in the standard heat transfer flow, for instance, water, lubricating oil, ethane-1,2 diols, and petrol. Many scholars have investigated the degree to which thermophysical characteristics of nanofluid boost heat dissipation by their scale, shape, concentrating, etc. The hollow cylindrical nanostructures are carbon nanofluids, whose walls are constructed from dense carbon sheets. (CNTs) are known as walled single nanotubes and wall-mounted nanotubes. CNTs have usually lots of processing and biomedical applications while the most critical function of nanotubes in fluid dynamics is the control of heat transfer to fluids [1]. In various engineering and science fields, the theory for boundary layers plays an important role. The boundary layer flow of a single-walled carbon nanotube nanofluid approaching three nonlinear thin isothermal needles of paraboloid, cone, and cylinder shapes with convective boundary conditions is predicted in [2] using an artificial neural network (ANN). Under the phenomenon of zero heat and mass flux, a single and dual phase technique is employed to build the management model. In ref [3], the role of Casson carbon nanotubes in boundary layer flow is being studied, having implications for both single-walled and multiwalled CNTs. The rate of heat transmission is examined under convective conditions. Various studies of nanofluid boundary layer motion around a wedge have been found in the literature. Khan and Pop [4] numerically analyzed the flow of the nanofluid limit layer through a wedge. The thermal radiation, viscose dissipation, and chemical reactions of MHD boundary layer nanofluid flow by the wedge were investigated by Pandy and Kumar [5]. Flows past a wedge could be used in polymer processing, crude oil extraction, the flow of molten metals over ramped surfaces, liquid metal flows in heat exchangers, the throwing

of chilled air through AC panels, nuclear power plants, designing flaps on aeroplane wings for increased lift, drag, and maneuverability, modeling of warships and submarines, and a variety of other scientific and engineering fields. Many scholars have recently shown a strong interest in studying fluid flow past a wedge surface.

The irreversibility of simple heat transfer methods is assessed using the Second Thermodynamics Law. Entropic generation is studied to understand the connection between thermal energy and other energy types that influence process matter. Malvandi et al. [6] are investigating the formation of entropy in nanofluid on a flat plate.

In recent decades, the issue of MHD and nanofluid has become more industrial. Initially, the magnetic field's influence on the convection of natural heat transfer was investigated by Sparrow and Cess. The hydromagnetic flow and heat transport through the stretching layer have been investigated by Chakrabarti and Gupta [7]. Casson nanofluids, which belong to the class of non-Newtonian fluids, have rheological properties in the shear stress-strain relationship. These are routinely used in several processes in engineering and technology [8].

More than one paper was then flooded and extensively discussed in the field of nanofluid science. The transmission of heat with fluid particulate suspension was documented under Saeed et al. [9]. At the melting heat transfer to the boundary nanofluid fluid layer stagnation point on to the stretching shrinking sheet, Kumar and Bandari [10] were recently noted. Features of double stratification on stagnation point flow of Walter's B nanoliquid driven through Riga surface are examined in [11]. Via solutal stratification, radiation, and thermal effects, heat and mass phenomena are examined.

The limit layer flow was observed by Yacob et al. [12] past a deteriorating/decreasing surface in nanofluid under an external, consistent shear flow with a convective surface border status. The MHD-forced layer flow of $Al_2O_3 - H_2O$ nanofluid over a flat, motionless plate with convective surface configuration was observed [13].

The intensive nanofluid study has undergone significant advances and is applied to various surfaces, sizes, and conditions by numerous researchers. The MHD convection and thermal transfer over the inclined cylinder were investigated by Dhanai et al. [14] for velocity and thermal slip effects: $Al_2O_3 - H_2O$. Nanofluid force convection in a nanoparticle was observed by the Malvandi and Ganji [15].

The study of 3D flows is mentioned in comparison to two-dimensional flows. The physical question is better known. The 3D boundary layer flow caused by the extension layer was addressed by Wang [16]. Different types of papers were suggested for 3D flow accordingly. The three-dimensional nanofluid flow model with the use for solar energy was explored by Ahmad Khan et al. [17]. Some recent demonstration on flow in circular rings and circular cylinder can be seen in [18, 19].

At its general three-dimensional stagnation, Bachok et al. [20] investigate the flow and heat transfer of nanofluid. The 3D hydromagnetic point flow of stagnation to a heat generating layer was addressed by Attia [21]. Mansur and Ishak [22] depicted the nanofluid three-dimensional fluid flow and thermal transmission across a permeable, convective boundary layer.

Khan et al. [23] convected exponentially expanded layers to computer analysis of the 3D nanofluid flow. Hayat et al. [24] have been studying 3D magneto-hydrodynamic nanofluid flow with slip speed and nonlinear thermal radiation. The role of nanoparticle aggregation kinetics in thermal conductivity is experimentally recognized by Prasher [25]. Chen et al. [26] recorded entropy characteristics to include titanium particles. They used the nanoparticle aggregation mechanism to predict thermal conductivity. Zhou and Keller [27] used ZnO to describe the effect of the fractal component of the nanoparticle aggregation. They showed the effect of pH on the phenomenon of aggregation. Mahanthesh et al. [28] investigated the kinematics of nanoparticle aggregation by using modified models for thermal conductivity and dynamic viscosity developed by Maxwell–Bruggeman and Krieger–Dougherty. Sedighi and Mohebbi [29] have investigated the thermal conductivity and basic heat characteristics of nanolithic aggregations by adding nanoparticles. Heris et al. [30] conducted an inspection on ZnO nanolubricants. The development of nanoparticle aggregation in the base fluid was demonstrated by the correlation of Krieger and Dougherty. Chen et al. [31] conducted a comprehensive study on impact of the nanoparticle aggregation on the nanofluid's radiative properties. The increment of viscosity nanoparticle aggregation was reported by He et al. [32].

In physics and engineering challenges, heat transmission is crucial. The influence of Newtonian heating on nanofluid flow over a nonlinear permeable stretching/shrinking sheet towards the stagnation point is investigated in this work. In the heat transfer process, entropy generation analysis also plays a vibrant role. Entropic scrutiny is focused on irreversibility of the thermal system. Any thermal and heat transfer equipment, including the heat exchanger and heat sink, shall obey the irreversibility. The source of irreversibility should be established and to some degree minimized. Mustafa et al. [33] investigated the generation of entropy by nanofluid flow in the vertical microchannel. They found that the number of grash increases the rate of entropy. A porous Al_2O_3/water fluid phase has been shown by Makinde and Eegunjobi [34]. They found that the nanoparticle concentration in Bejan increased.

The thermal characteristics that define the physical situation have often been challenged by scientists and inventors. Ibanez et al. investigated entropy generation using the separate flow model in a nanofluid-driven microchannel. The MHD nanofluid stream over L-shaped ribs was examined by Torabi et al. [35]. Toghraie et al. [36] use the spectral quasilinearization (SQLM) approach to solve the complex differential equations that govern nonlinear mixed convective heat transfer of a Williamson fluid down a vertical microchannel. They demonstrated that the boundary conditions of convection heating at the microchannel walls cause the most entropy formation.

The present article addresses the entropy generation of internal layer flow and MWCNT-containing nanofluid thermal transmission. In this research project, the uniqueness

and impact of nanoparticles, convective surfaces, and heat radiation are calculated. The solutions are obtained by numerical calculation. In both situations, the physical effects of nanofluid flow, i.e., (i) without aggregating the nanoparticles and (ii) with nanoparticles, are examined.

The main objectives of this work are as follows.

(i) The characteristics of flow and thermal field are interpreted and missing by filming with nanofluid aggregation

(ii) Examine the heat transfer phenomenon root of irreversibility

(iii) Find out which physical factor contributes to the generation of entropy

(iv) Find out how entropy production can be minimized by manipulating flow parameters

2. Description of the Model

Consider a two-dimension, laminar, steady, incompressible nanofluids of viscous flow through a wedge in a stream of water-based nanofluid containing multiwall CNT (see Figure 1). The set of Cartesian coordinates is used in the problem under consideration. The lower surface of the wedge is supposed to be heated by convection from a hot fluid at a temperature Tf that yields the heat transfer coefficient hf. The nanoparticles and the base fluid (water) are also considered to be in equilibrium, with no slip between them.

The equations that govern the nanofluid model over wedge geometry was described in the following form [37]:

$$\frac{\partial u}{\partial x} + \frac{\partial v}{\partial y} = 0,$$
$$u\frac{\partial u}{\partial x} + v\frac{\partial u}{\partial y} = U_\infty \frac{\partial U_e}{\partial x} + \frac{\mu_{nf}}{\rho_{nf}}\frac{\partial^2 u}{\partial y^2},$$
$$u\frac{\partial T}{\partial x} + v\frac{\partial T}{\partial y} = \alpha_{nf}\frac{\partial^2 T}{\partial y^2} + \frac{\mu_{nf}}{(\rho C_p)_{nf}}\left(\frac{\partial u}{\partial y}\right)^2 - \frac{1}{(\rho C_p)_{nf}}\frac{\partial q_r}{\partial y}, \tag{1}$$

where u and v represent the components of velocity in the x and y direction of the fluid flows, respectively. The coordinate system and problem geometry are described in Figure 1. T represents the temperature of nanofluid. Furthermore, μ_{nf} and ρ_{nf} are the dynamic nanofluids viscosity and density, and σ_{nf} is the thermal diffusivity of the nanofluid.

2.1. Thermal Physical Characteristics of Nanofluids

2.1.1. The Conventional Model without Aggregation (Case 1). The productive hybrid nanofluid density ρ_{nf} and capacity of heat $((\rho C_p)_{nf})$ are defined by

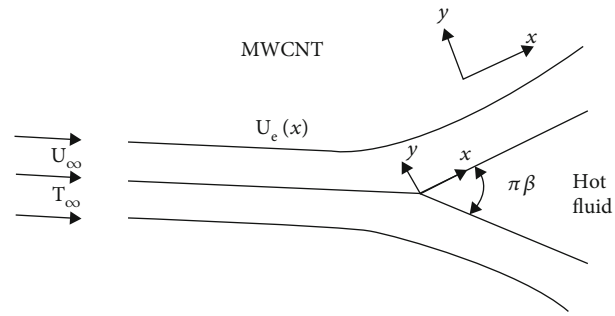

Figure 1: Physical model of the problem.

$$(\rho C_p)_{nf} = (1-\phi)(\rho C_p)_f + \phi(\rho C_p)_s, \rho_{nf} = (1-\phi)\rho_f + \phi\rho_s, \tag{2}$$

where ϕ is a nanofluid fixed volume fraction. The nanofluid dynamic viscosity is calculated as [38]

$$\frac{\mu_{nf}}{\mu_f} = \frac{1}{(1-\phi)^{2.5}}. \tag{3}$$

The effective nanofluid thermal conductivity is determined by

$$\frac{k_{nf}}{k_f} = \frac{k_s + 2k_f - 2\phi(k_f - k_s)}{k_s + 2k_f + \phi(k_f - k_s)}, \tag{4}$$

where k_{nf} is the nanofluid thermal conductivity, and k_f is the thermal conductivity of base fluid. Recommended boundary conditions are implemented through the disk as

$$u = 0, v = 0, -k_{nf}\frac{\partial T}{\partial y} = h_f(T_f - T), \text{at } y = 0,$$
$$u = U_e(x) = U_\infty x^m, v = 0, T = T_\infty, \text{at } y \longrightarrow \infty. \tag{5}$$

2.1.2. The Conventional Model with Aggregation (Case 2). The fluid model, for example, Brinkman, Einstein, and Maxwell, depends only on the fraction of the nanoparticle volume. The nanofluid's normalized shear viscosity does not depend on the temperature. The model of aggregation clarifies these features. In addition, nanofluid thermal conductivity is higher with experimental results than with common fluid models. This difference is explained by the neglected effect of nanoparticles [9, 10]. Therefore, consideration of the film aggregation of nanoparticles is necessary to explore the ratio of thermal conductivity. Thermophysical properties of base fluid and

nanoparticles are given in Table 1.

$$\begin{aligned}\rho_{nf} &= (1-\phi_a)\rho_f + \phi_a\rho_s,\\ \frac{\mu_{nf}}{\mu_f} &= \left(1-\frac{\phi_a}{\phi_m}\right)^{[\eta]\phi_m},\\ (\rho C_p)_{nf} &= (1-\phi_a)(\rho C_p)_f + \phi_a(\rho C_p)_s,\\ \frac{k_{nf}}{k_f} &= \frac{k_a+2k_f-2\phi_a(k_f-k_a)}{k_a+2k_f+\phi_a(k_f-k_a)},\end{aligned} \tag{6}$$

where ϕ_m is an extreme fraction of the volume, $[\eta]$ is an Einstein coefficient, and ϕ_a is an effective fraction of the volume of the aggregates.

$$\phi_a = \phi\left(\frac{r_a}{r_p}\right)^{3-D}. \tag{7}$$

Experimental values are very well agreed with the commonly accepted values $D = 1.8$, $(r_a/r_p) = 3.34$, $\phi_m = 0.605$, and $[\eta] = 2.5$. Nanoparticle aggregation is included in the thermal conductivity deduction by Bruggeman:

$$\begin{aligned}\frac{k_{nf}}{k_f} = \frac{1}{4}\Bigg\{&(3\phi_m-1)\frac{k_s}{k_f} + (3(1-\phi_m)-1)\\ &+\left[\left((3\phi_{\text{in}}-1)\frac{k_s}{k_f}+(3(1-\phi_{\text{in}})-1)\right)^2 + 8\frac{k_s}{k_f}\right]\Bigg\},\end{aligned}$$

$$\phi_{\text{in}} = \left(\frac{r_a}{r_p}\right)^{D-3}. \tag{8}$$

By using similarity transformations,

$$\eta = \left(\frac{(\text{m}+1)U_e(x)}{2\upsilon_{bf}x}\right)^{1/2} y,\ u = U_e(x)f'(\eta),$$

$$\theta(\eta) = \frac{(T-T_\infty)}{(T_w-T_\infty)},\ v = \left(\frac{(\text{m}+1)\upsilon_{bf}U_e(x)}{2x}\right)^{1/2}\left[f + \left(\frac{(m-1)}{(m+1)}\right)\eta f'(\eta)\right]. \tag{9}$$

Substituting values to get

$$f''' + (1-\phi)^{2.5}\left(1-\phi+\phi\frac{\rho_{nf}}{\rho_f}\right)\left[ff'' + \frac{(2m)}{(m+1)}\left(1-f'^2\right)\right] = 0, \tag{10}$$

$$\left(\frac{k_{nf}}{k_f}+\frac{4}{3Nr}\right)\theta'' + \left(1-\phi+\phi\rho_{nf}/\rho_f\right)\text{Pr}\, f\,\theta' + \frac{Br}{(1-\phi)^{2.5}}f''^2 = 0, \tag{11}$$

where N_r is the radiation parameter, and $\text{Br} = \text{Pr.Ec}$ (where Ec represents the Eckert number) is the Brinkman number. Bi is the surface convection parameter, $\text{Pr} = \nu_f/\alpha_f$ is the Prandtl number, and primes signify derivative w.r.t η. The modified BCs transform into

$$f(0) = 0, f'(0) = 0, \theta'(0) = -Bi(1-\theta(0)), \tag{12}$$

$$f'(\eta) = 1, \theta(\eta) = 0\ as\ (\eta) \longrightarrow \infty. \tag{13}$$

2.2. Entropy Generation. Entropy generation includes the existing irreversibility of the physical phenomenon. The term entropy is used

$$S_g = \frac{k_{nf}}{T_\infty^2}\left[\left(\frac{\partial T}{\partial y}\right)^2 + \frac{16\sigma^* T_\infty^2}{3k_{bf}k^*}\left(\frac{\partial T}{\partial y}\right)^2\right] + \frac{\mu_{nf}}{T_\infty}\left(\frac{\partial u}{\partial y}\right)^2 = 0. \tag{14}$$

The nondimensional entropy generation is given by

$$N_s = \frac{S_g}{S_{g0}} = \left(\frac{m+1}{2}\right)\text{Re}_x\left[\frac{k_{nf}}{k_{bf}}\left(1+\frac{4}{3Nr}\right)\theta'^2 + \frac{Br}{\Omega(1-\phi)^{2.5}}\left(f''\right)^2\right], \tag{15}$$

where $S_{g0} = (k_{bf}\Delta T^2/T_\infty^2 x^2)$ is the characteristic entropy generation rate, and $\Omega^{-1} = T_\infty/\Delta T$ is the dimensionless temperature difference.

Table 2 shows the comparison between results of previous publications [39, 40] and some of our results with a perfect agreement.

We are introducing the Bejan number (Be) as the ratio between entropy and total entropy output induced by heat transfer.

$$\text{Be} = \frac{\text{Entropy genration due to heat transfer}}{\text{Total entropy generation}}. \tag{16}$$

If Be = 1 dominates irreversibility in heat transfers, while Be = 0 dominates irreversibility as a result of fluid friction, Be = 1/2 dominates when fluid rubbing, and heat transfers are irreversible.

2.2.1. Mathematical Analysis. Equations (10) and (11) relative to equation (12) are combined with nonlinear DEs to be numerically solved by Runge-Kutta-Fehlberg scheme for differential values of physical parameters. In order to obtain the numerical approaches, the governing nonlinear ODEs (10) and (11) and BCs (12) transformed to a number of simultaneous DEs of the first order.

Table 1: Thermal physical characteristics of H_2O and MWCNT [31].

Physical properties	$\rho\left(\frac{kg}{m^3}\right)$	$C_p\left(\frac{J}{kg}K\right)$	$k\left(\frac{W}{m}K\right)$
Pure water (H_2O)	997.0	4179	0.613
MWCNT	1600	796	3000

Table 2: Comparison between present result and Ref [39, 40].

m	Yih [36]	White [37]	Present
0	0.4696	0.4696	0.4696
$\frac{1}{11}$	0.6550	0.6550	0.6550
$\frac{1}{5}$	0.8021	0.8021	0.8021
$\frac{1}{3}$	0.9276	0.9276	0.9277

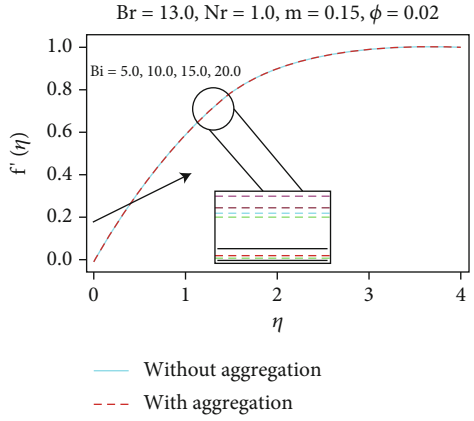

Figure 2: Impact of Bi parameter on $f'(\eta)$.

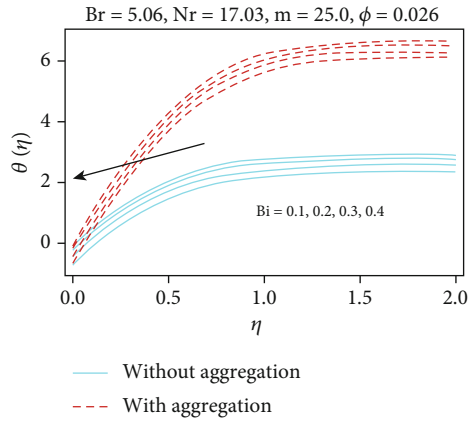

Figure 3: Impact of Bi parameter on $\theta(\eta)$.

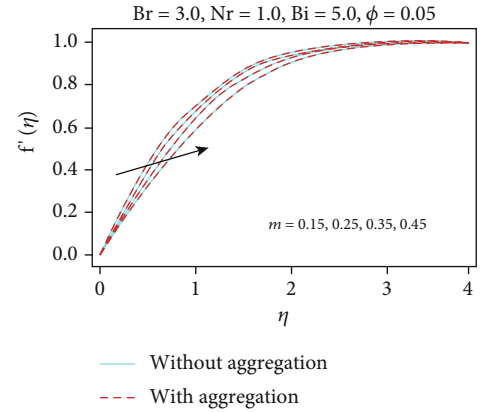

Figure 4: Impact of m parameter on $f'(\eta)$.

3. Interpretations of the Results

In the presence of thermal radiation, the numerical results for entropy production inside the nanofluid border layer over the wedge are graphically represented. The results show extraordinary agreement and therefore trust us to use the current code. For certain values of (Bi), m, Nr, Br, and ϕ, the nonlinear ordinary differential equations (10) and (11) subject to boundary condition (12) is numerically solved. Many kinds of nanoparticles are considered that are the fluid of base Cu, CuO,Al_2O_3, and H_2O. Let us take into account of the value (Pr) of 6.2 for the current analysis.

The impact of Bi for the velocity component $f'(\eta)$ and the field of temperature, $\theta(\eta)$, respectively, are shown in Figures 2 and 3. Biot number is a dimensional quantity comparing relative external and internal resistance transmission. The heated fluid heats up the lower surface of the stretch sheet as Bi rises, causing convective heat to be transferred. As a result of the rise in the number of Biot, the temperature increases. Eventually, it increases the thickness of the thermal boundaries. It is important to note that the inclusion of nanoparticle aggregation leads to an enhanced temperature profile.

For velocity components $f'(\eta)$ and the distribution of the temperature field $\theta(\eta)$, respectively, the effects of the m parameter are shown in Figures 4 and 5. The findings are very much in agreement. The $f'(\eta)$ values are reduced and for the larger m,$\theta(\eta)$ increases. Physically, the increment in $\theta(\eta)$ is due to the resistive force that occurs from the magnetic field. The Lorentz force, which is induced by the magnetic field, is the physical reason behind this. Figures 6 and 7 display the effect of Nr on $f'(\eta)$ and $\theta(\eta)$ temperature. $f'(\eta)$ decreases and increases the thickness of thermal boundary layer as Nr increases. Figures 8 and 9 show that with the rise in ϕ, both the velocity profile $f'(\eta)$ and the distribution of the temperature field $\theta(\eta)$ increase. Physically, this is due to increased dynamic viscosity and increased momentum diffusion. The increase in the thermal conductivity of the nanoliquid is attributable to the existence of more nanoparticles. The fluid close to the nanoparticles forms a nanolayer

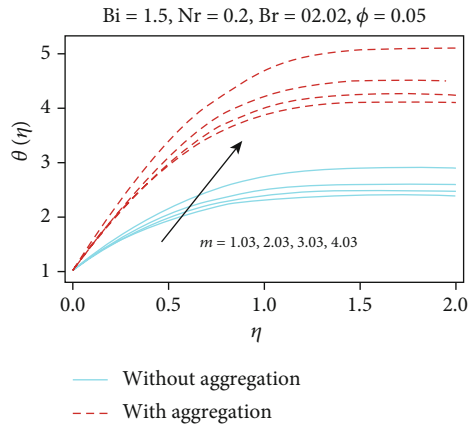

Figure 5: Impact of m parameter on $\theta(\eta)$.

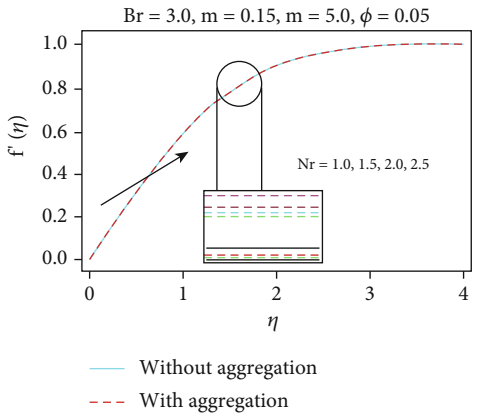

Figure 6: Impact of Nr parameter on $f'(\eta)$.

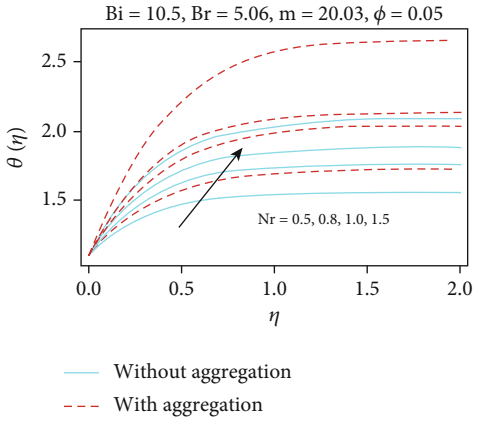

Figure 7: Impact of Nr parameter on $\theta(\eta)$.

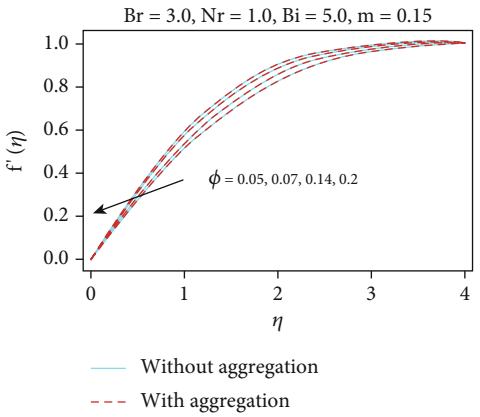

Figure 8: Impact of ϕ parameter on $f'(\eta)$.

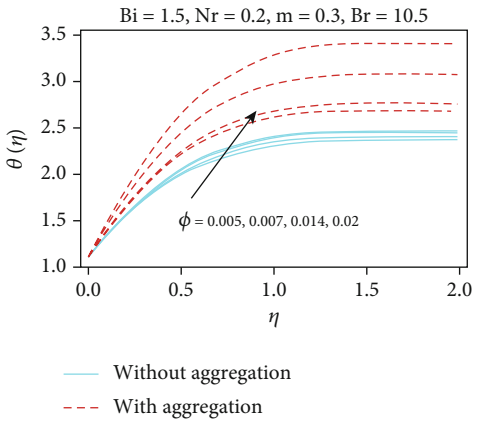

Figure 9: Impact of ϕ parameter on $\theta(\eta)$.

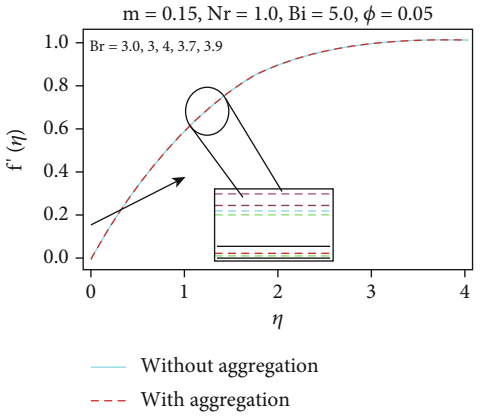

Figure 10: Impact of Br parameter on $f'(\eta)$.

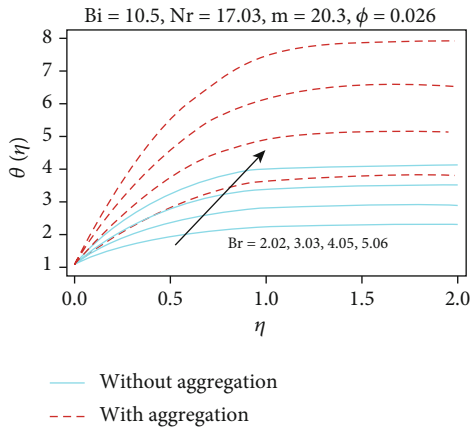

Figure 11: Effect of Br on $\theta(\eta)$.

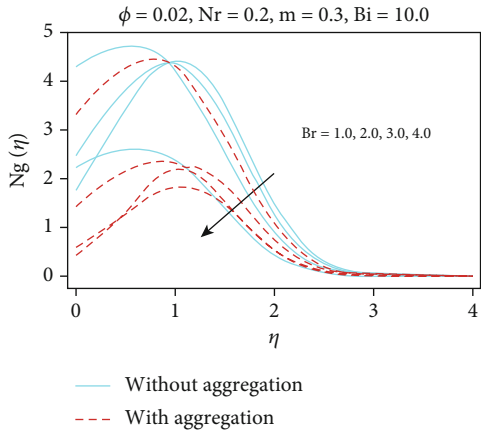

Figure 12: Effect of Bi parameter on Ng (η).

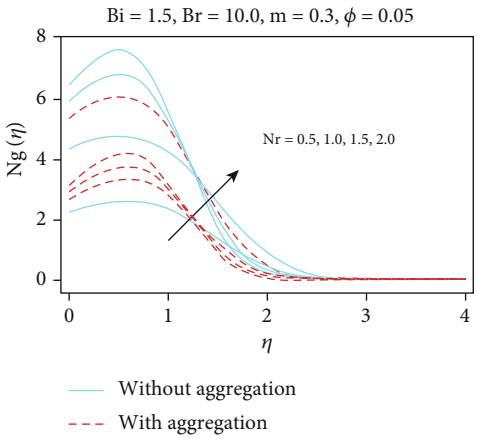

Figure 13: Impact of Nr parameter on Ng (η).

since the nanoparticles are formed and serve as a bridge between the particles and the fluid aggregates. The density of the nanolayer plays an important part in improving thermal conductivity. This nanolayer plays an important role in the transmission of heat from solid to nearby liquid.

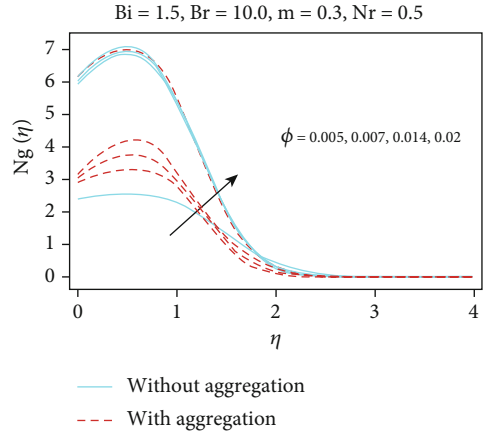

Figure 14: Impact of ϕ parameter on Ng (η).

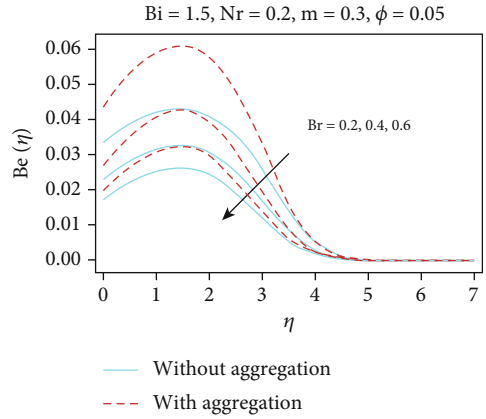

Figure 15: Impact of Br parameter on Be (η).

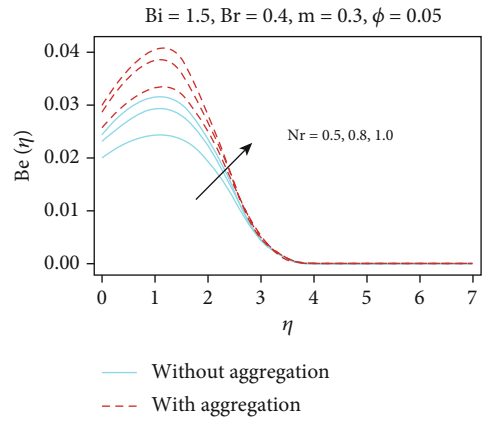

Figure 16: Impact of Nr parameter on Be (η).

Br effects are shown in Figures 10 and 11 for $f'(\eta)$ and $\theta(\eta)$. It seems that $f'(\eta)$ decreases, and the thermal limit thickness increases with Br. The effect of Bi, Nr, and ϕ nanoparticles on $Ng(\eta)$ is shown in Figures 12–14. It is evident that with higher ϕ, $Ng(\eta)$ decreases and Bi increases. Increased

radiation parameters in $Ng(\eta)$ and Nr continue to increase the entropy generation. This action of entropy generation is motivated by a reduction in the radiation absorption rate. Therefore, the best way to reduce entropy production is to increase the radiation parameter. It is illustrated that the nanoparticle aggregation model has a lower entropy generation.

The Bejan number for parameters ϕ, Nr, and Br is shown in Figures 15 and 16. The $\mathrm{Be}(\eta)$ curve tends to increase until the maximum value is reached first and then begins to decrease unless the value is zero. It is observed that the number of Bejan increases to increase the value of Nr. The maximum value of $\mathrm{Be}(\eta)$ is increased with greater Nr and decreased with ϕ and Br. It is known from these graphs that the number of Bejan is greater for the aggregation model.

4. Conclusions

This study develops a mathematical expression for the entropy processing and heat transfer studies of MWCNT-containing incompressible nanofluids under the conditions of convective conditions and nanofluid thermal radiation. A cinematic aggregation model for the analysis of nanoliquid flow is considered. The significance of the different speed profile parameters, thermal profile, entropy generation, and the number of Bejan is considered. The following fundamental conclusions are drawn from the current study:

(i) The increase in volume phi and Biot Bi fraction increases thickness of temperature but decreases the radiation parameter

(ii) It is noted that the aggregation model has a higher temperature profile than traditional models

(iii) Entropy production increases in nanofluid for a wider volume fraction of nanoparticles

(iv) The entropy production is reduced in the aggregation model of nanoparticles

(v) The reduction of entropy can be achieved by increasing the radiation parameter and reducing crossborder convection

(vi) Nanofluid entropy production increases for higher volume fraction values

(vii) The number Bejan is increased with the radiation parameter and the number Biot

(viii) It has been emphasized that a model of aggregation of nanoparticles shows a higher number Bejan

Nomenclature

u: Component of velocity in the x direction
v: Component of velocity in the y direction
μ: Dynamic viscosity
ν: Kinematics viscosity
Re: Local Reynolds number
T: Surface temperatures
T_∞: Environmental temperatures
$(\rho Cp)_{nf}$: Nanofluid heat power
ρ_{nf}: Density of nanofluid
ρs: Density of solid particle
ϕ: Volume fraction of nanoparticles
kf: Conductivity of the base fluid
θ: Dimensionless temperature
η: Dimensionless variable
Nu: Nusselt number
Pr: Prandtl number
q_r: Rosseland approximation
Ec: Eckert number
N: Radiation parameter
N_g: Entropy generation
Be: Bejan number
Ω: Thermal difference parameter
k_a: Thermal conductivity of the aggregates
ϕ_a: Volume fraction of nanoparticle aggregates
ϕ_m: Maximum volume fraction of nanoparticles
r_a, r_p: Radii of aggregates and nanoparticles.

Data Availability

No data were used in the presented work.

Conflicts of Interest

The authors declare that there is no financial/competing interest regarding to this work.

References

[1] Y. Ding, H. Alias, D. Wen, and R. A. Williams, "Heat transfer of aqueous suspensions of carbon nanotubes (CNT nanofluids)," *International Journal of Heat and Mass Transfer*, vol. 49, no. 1-2, pp. 240–250, 2006.

[2] A. Shafiq, A. B. Çolak, and T. Naz Sindhu, "Designing artificial neural network of nanoparticle diameter and solid–fluid interfacial layer on single-walled carbon nanotubes/ethylene glycol nanofluid flow on thin slendering needles," *International Journal for Numerical Methods in Fluids*, vol. 93, no. 12, pp. 3384–3404, 2021.

[3] A. Shafiq, T. N. Sindhu, and Q. M. Al-Mdallal, "A sensitivity study on carbon nanotubes significance in Darcy–Forchheimer flow towards a rotating disk by response surface methodology," *Scientific Reports*, vol. 11, no. 1, pp. 1–26, 2021.

[4] W. A. Khan and I. Pop, "Boundary layer flow past a wedge moving in a nanofluid," *Mathematical Problems in Engineering*, vol. 2013, Article ID 637285, 7 pages, 2013.

[5] A. K. Pandey and M. Kumar, "Chemical reaction and thermal radiation effects on boundary layer flow of nanofluid over a wedge with viscous and Ohmic dissipation, *St. Petersburg Polytechnical University*," *Journal of Physics and Mathematics*, vol. 3, pp. 322–332, 2017.

[6] A. Malvandi, D. D. Ganji, F. Hedayati, and E. Yousefi Bar, "An analytical study on entropy generation of nanofluids over a flat plate," *Journal of Alexandria Engineering*, vol. 52, no. 4, pp. 595–604, 2013.

[7] A. Chakrabarti and A. S. Gupta, "Hydromagnetic flow and heat transfer over a stretching sheet," *Quarterly Journal of Mechanics and Applied Mathematics*, vol. 37, pp. 73–78, 1979.

[8] M. Bilal, A. Saeed, T. Gul, I. Ali, W. Kumam, and P. Kumam, "Numerical approximation of microorganisms hybrid nanofluid flow induced by a wavy fluctuating spinning disc," *Coatings*, vol. 11, no. 9, p. 1032, 2021.

[9] A. Saeed, P. Kumam, T. Gul, W. Alghamdi, W. Kumam, and A. Khan, "Darcy–Forchheimer couple stress hybrid nanofluids flow with variable fluid properties," *Scientific Reports*, vol. 11, no. 1, pp. 1–13, 2021.

[10] A. Saeed, P. Kumam, S. Nasir, T. Gul, and W. Kumam, "Nonlinear convective flow of the thin film nanofluid over an inclined stretching surface," *Scientific Reports*, vol. 11, no. 1, pp. 1–15, 2021.

[11] A. Shafiq, F. Mebarek-Oudina, T. N. Sindhu, and A. Abidi, "A study of dual stratification on stagnation point Walters' B nanofluid flow via radiative Riga plate: a statistical approach," *The European Physical Journal Plus*, vol. 136, no. 4, pp. 1–24, 2021.

[12] N. A. Yacob, A. Ishak, I. Pop, and K. Vajravelu, "Boundary layer flow past a stretching/shrinking surface beneath an external uniform shear flow with a convective surface boundary condition in a nanofluid," *Nanoscale Research Letters*, vol. 6, no. 1, p. 314, 2011.

[13] J. Bouslimi, M. A. Abdelhafez, A. M. Abd-Alla, S. M. Abo-Dahab, and K. H. Mahmoud, "MHD mixed convection nanofluid flow over convectively heated nonlinear due to an extending surface with Soret effect," *Complexity*, vol. 2021, Article ID 5592024, 20 pages, 2021.

[14] R. Dhanai, P. Rana, and L. Kumar, "MHD mixed convection nanofluid flow and heat transfer over an inclined cylinder due to velocity and thermal slip effects: Buongiorno's model," *Powder Technology*, vol. 288, pp. 140–150, 2016.

[15] A. Malvandi and D. D. Ganji, "Effects of nanoparticle migration on force convection of alumina/water nanofluid in a cooled parallel-plate channel," *Advanced Powder Technology*, vol. 25, no. 4, pp. 1369–1375, 2014.

[16] C. Wang, "The three-dimensional flow due to a stretching flat surface," *Physics of Fluids*, vol. 27, no. 8, pp. 1915–1917, 1984.

[17] J. A. Khan, M. Mustafa, T. Hayat, M. A. Farooq, A. Alsaedi, and S. Liao, "On model for three-dimensional flow of nanofluid: an application to solar energy," *Journal of Molecular Liquids*, vol. 194, pp. 41–47, 2014.

[18] A. A. Memon, M. A. Memon, K. Bhatti, K. Nonlaopon, and I. Khan, "Simulation of non-isothermal turbulent flows through circular rings of steel," *CMC-Computers Materials & Continua*, vol. 70, no. 3, pp. 4341–4355, 2022.

[19] A. A. Memon, M. A. Memon, K. Bhatti, T. A. Alkanhal, I. Khan, and A. Khan, "Analysis of power law fluids and the heat distribution on a facing surface of a circular cylinder embedded in rectangular channel fixed with screen: a finite element's analysis," *IEEE Access*, vol. 9, pp. 74719–74728, 2021.

[20] N. Bachok, A. Ishak, R. Nazar, and I. Pop, "Flow and heat transfer at a general three-dimensional stagnation point in a nanofluid," *Physics B*, vol. 405, no. 24, pp. 4914–4918, 2010.

[21] H. A. Attia, "Steady three-dimensional hydromagnetic stagnation point flow towards a stretching sheet with heat generation," *Italian Journal of Pure and Applied Mathematics*, vol. 27, pp. 9–18, 2010.

[22] S. Mansur and A. Ishak, "Three-dimensional flow and heat transfer of a nanofluid past a permeable stretching sheet with a convective boundary condition," *AIP Conf. Proc.*, vol. 1614, pp. 906–912, 2014.

[23] J. A. Khan, M. Mustafa, T. Hayat, and A. Alsaedi, "Numerical study on three-dimensional flow of nanofluid past a convectively heated exponentially stretching sheet," *Canadian Journal of Physics*, vol. 93, no. 10, pp. 1131–1137, 2015.

[24] T. Hayat, M. Imtiaz, A. Alsaedi, and M. A. Kutbi, "MHD three-dimensional flow of nanofluid with velocity slip and nonlinear thermal radiation," *Journal of Magnetism and Magnetic Materials*, vol. 396, pp. 31–37, 2015.

[25] R. Prasher, P. E. Phelan, and P. Bhattacharya, "Effect of aggregation kinetics on the thermal conductivity of nanoscale colloidal solutions (nanofluid)," *Nano Letters*, vol. 6, no. 7, pp. 1529–1534, 2006.

[26] H. Chen, Y. Ding, Y. He, and C. Tan, "Rheological behaviour of ethylene glycol based titania nanofluids," *Chemical Physics Letters*, vol. 444, no. 4-6, pp. 333–337, 2007.

[27] D. Zhou and A. A. Keller, "Role of morphology in the aggregation kinetics of ZnO nanoparticles," *Water Research*, vol. 44, no. 9, pp. 2948–2956, 2010.

[28] B. Mahanthesh, N. Srikantha, and J. Mackolil, "A study on heat transfer in three-dimensional nonlinear convective boundary layer flow of nanomaterial considering the aggregation of nanoparticles," *Heat Transfer*, vol. 51, no. 1, pp. 891–908, 2022.

[29] M. Sedighi and A. Mohebbi, "Investigation of nanoparticle aggregation effect on thermal properties of nanofluid by a combined equilibrium and non-equilibrium molecular dynamics simulation," *Journal of Molecular Liquids*, vol. 197, pp. 14–22, 2014.

[30] S. Z. Heris, M. A. Razbani, P. Estelle, and O. Mahian, "Rheological behavior of zincoxide nanolubricants," *Journal of Dispersion Science and Technology*, vol. 36, no. 8, pp. 1073–1079, 2015.

[31] J. Chen, C. Y. Zhao, and B. X. Wang, "Effect of nanoparticle aggregation on the thermal radiation properties of nanofluids: an experimental and theoretical study," *International Journal of Heat and Mass Transfer*, vol. 154, article 119690, 2020.

[32] Y. He, Y. Jin, H. Chen, Y. Ding, D. Cang, and H. Lu, "Heat transfer and flow behaviour of aqueous suspensions of TiO2 nanoparticles (nanofluids) flowing upward through a vertical pipe," *International Journal of Heat and Mass Transfer*, vol. 50, no. 11-12, pp. 2272–2281, 2007.

[33] I. Mustafa, T. Javed, A. Ghaffari, and H. Khalil, "Enhancement in heat and mass transfer over a permeable sheet with Newtonian heating effects on nanofluid: multiple solutions using spectral method and stability analysis," *Pramana*, vol. 93, no. 4, pp. 1–13, 2019.

[34] O. D. Makinde and A. S. Eegunjobi, "Entropy generation in a couple stress fluid flow through a vertical channel filled with saturated porous media," *Entropy*, vol. 15, no. 12, pp. 4589–4606, 2013.

[35] M. Torabi, S. M. Ghiaasiaan, and G. P. Peterson, "The effect of Al_2O_3-water nanofluid on the heat transfer and entropy generation of laminar forced convection through isotropic porous media," *nternational Journal of Heat and Mass Transfer*, vol. 111, pp. 804–816, 2017.

[36] D. Toghraie, M. Mahmoudi, O. A. Akbari, F. Pourfattah, and M. Heydari, "The effect of using water/CuO nanofluid and L-shaped porous ribs on the performance evaluation criterion of microchannels," *Journal of Thermal Analysis and Calorimetry*, vol. 135, no. 4, pp. 145–159, 2018.

[37] B. Mahanthesh, C. Srinivas Reddy, N. Srikantha, and G. Lorenzini, "Entropy generation analysis of radiative heat transfer in Williamson fluid flowing in a microchannel with nonlinear mixed convection and joule heating," *Proceedings of the Institution of Mechanical Engineers, Part E: Journal of Process Mechanical Engineering*, 2022.

[38] A. Zeeshan, M. Hassan, R. Ellahi, and M. Nawaz, "Shape effect of nanosize particles in unsteady mixed convection flow of nanofluid over disk with entropy generation," *Proceedings of the Institution of Mechanical Engineers, Part E: Journal of Process Mechanical Engineering*, vol. 231, no. 4, pp. 871–879, 2016.

[39] D. Lu, Z. Li, M. Ramzan, A. Shafee, and J. D. Chung, "Unsteady squeezing carbon nanotubes based nano-liquid flow with Cattaneo-Christov heat flux and homogeneous–heterogeneous reactions," *Applied Nanoscience*, vol. 9, no. 2, pp. 169–178, 2019.

[40] K. A. Yih, "Uniform suction/blowing effect on forced convection about a wedge: uniform heat flux," *Acta Mechanica*, vol. 128, no. 3-4, pp. 173–181, 1998.